Proceedings of Meetings on Acoustics

Volume 60 http://acousticalsociety.org/

Sixth Joint Meeting

189th Meeting of the Acoustical Society of America and the Acoustical Society of Japan

Honolulu, Hawaii
1-5 December 2025

Computational Acoustics: Paper 4aCA4

Time-domain simulation tool with a graphical interface for modeling nonlinear waves with shocks in weakly absorptive media

Maria S. Sergeeva, Anastasia V. Kvashennikova, and Vera A. Khokhlova
Laboratory for Industrial and Medical Ultrasound, Faculty of Physics, Lomonosov Moscow State University, Moscow, 119991, RUSSIA; s_masha_ss@mail.ru; kvashennikovaav@my.msu.ru; vera@acs366.phys.msu.ru

William A. Willis
Walker Department of Mechanical Engineering, The University of Texas at Austin, Austin, Texas, 78712-1063, USA; william.willis@utexas.edu

John M. Cormack
Division of Cardiology, Department of Medicine, University of Pittsburgh, Pittsburgh, Pennsylvania, 15213, USA; jmc345@pitt.edu

Mark F. Hamilton
Walker Department of Mechanical Engineering, The University of Texas at Austin, Austin, Texas, 78712-1063, USA; hamilton@mail.utexas.edu

B-Sim is open-access MATLAB software with a graphical user interface (GUI) developed for modeling the nonlinear propagation of high-amplitude acoustic plane waves with shocks. It implements numerical solutions of the Burgers equation, accounting for the effects of nonlinearity and thermoviscous absorption. B-Sim enables a comparative analysis of four time-domain algorithms commonly used in nonlinear acoustics: a conservative scheme, a shock-capturing Godunov-type scheme, an algorithm based on the exact implicit solution of the lossless Burgers equation, and a scheme operating in intrinsic coordinates. The software allows for analysing nonlinear shock-wave propagation effects for several predefined initial waveforms as well as the efficiency, accuracy, limitations, and specific features of various time-domain numerical approaches. The software can be used for educational purposes as a supplement to courses on nonlinear and computational acoustics, and can also serve as a research tool for evaluating computational efficiency of the included algorithms when solving more general problems of nonlinear acoustics.

Proceedings of Meetings on Acoustics, Vol. 60, 022004 (2026); https://doi.org/10.1121/2.0002289.

1. INTRODUCTION

Nonlinear acoustic wave propagation effects are important in a wide range of practical problems including atmospheric and underwater acoustics, therapeutic ultrasound applications, and others.[1] Nonlinear propagation of high-amplitude acoustic waves is accompanied by distortion of the initial waveform, the subsequent generation of higher harmonics in the spectrum, and the formation of steep shocks.[2]

To simulate strongly nonlinear sound fields with shocks, evolution equations such as the Burgers equation[3] for plane waves and the one-way Westervelt equation[4] and Khokhlov–Zabolotskaya–Kuznetsov (KZK) equation[5] for diffracting waves are commonly used. These equations are typically solved using marching schemes with an operator splitting procedure,[6-10] which allows for modeling nonlinearity, diffraction, thermoviscous absorption, relaxation, and other wave effects using the most efficient algorithm for each effect. Because calculation of the nonlinear operator in strongly nonlinear regimes becomes particularly challenging, it is important to assess the effectiveness of the various numerical implementations. Frequency-domain methods[10-12] are inefficient because the number of operations is proportional to the number of harmonics squared,[6,13] and thousands of harmonics are required for an accurate representation of steep shocks. Thus, time-domain algorithms[7-9,14] are preferable, as their computational costs scale linearly with the number of time grid points.

A software package named B-Sim with a user-friendly interface has been developed to numerically simulate nonlinear acoustic fields with steep shocks based on the Burgers equation, which accounts for nonlinearity and thermoviscous absorption. The MATLAB graphical user interface (GUI) application is designed to illustrate specific features and compare the accuracy, limitations, and computational efficiency of four representative time-domain marching schemes: a conventional conservative finite-difference scheme;[15-17] a shock-capturing Godunov-type method;[18-22] an algorithm[7-9] based on the exact implicit solution of the lossless Burgers equation also known as the Riemann equation[2,23] with an interpolation procedure, which will be referred to as the Austin algorithm due to the location of its development; and an intrinsic coordinate (IC) scheme[24,25] that accounts for thermoviscous absorption by the equal area rule and was developed specifically for simulation including relaxation. This open-access software can be adapted to serve as a research tool for assessing more general nonlinear propagation problems with additional effects, such as diffraction, geometrical spreading, relaxation, and power law of absorption, which can be treated independently using the operator-splitting method. In addition, it can serve as an educational resource for courses in nonlinear acoustics, numerical methods, or wave physics. It provides an opportunity to assess the performance of each of these four algorithms for initial waveforms, periodic waves and single pulses, with both symmetric and moving shocks, allowing a comparative analysis in terms of achievable accuracy in governing steep shock fronts with the minimum required number of time points and the minimum run time.

2. NUMERICAL MODEL

A. BURGERS EQUATION

To simulate the effects of nonlinearity and thermoviscous absorption, the Burgers[3] equation is used as the theoretical model in B-Sim:

$$\frac{\partial p}{\partial z} = \frac{\beta}{\rho_0 c_0^3} p \frac{\partial p}{\partial \tau} + \frac{\delta}{2c_0^3} \frac{\partial^2 p}{\partial \tau^2}, \tag{1}$$

where p is the acoustic pressure, z is the propagation coordinate, $\tau = t - z/c_0$ is the retarded time, c_0 is the sound speed, ρ_0 is the density of the medium, and β and δ are the nonlinearity and thermoviscous absorption coefficients for the medium, respectively [see Eq. (3.54) in Ref. 2].

For the convenience of numerical modeling, the following dimensionless variables are introduced:

$$P = p/p_0, \quad \theta = \omega_0 \tau, \quad Z = z/l_{\mathrm{sh}}. \tag{2}$$

Here, p_0 and ω_0 are the characteristic peak pressure and frequency of the initial harmonic or pulsed waveform, respectively; $l_{\mathrm{sh}} = \rho_0 c_0^3/(\beta \omega_0 p_0)$ is the characteristic nonlinear length scale, e.g., the shock formation distance in case of the initially harmonic wave.

The Burgers equation (1) in dimensionless variables (2) then takes the form

$$\frac{\partial P}{\partial Z} = P \frac{\partial P}{\partial \theta} + A \frac{\partial^2 P}{\partial \theta^2}, \tag{3}$$

where the combined effects of nonlinearity and thermoviscous absorption depend on the single dimensionless parameter $A = \delta \rho_0 \omega_0/(2\beta p_0)$, which is equal to the ratio of the nonlinear length l_{sh} to the absorption length $l_{\mathrm{abs}} = 2c_0^3/(\delta \omega_0^2)$. Note that the regime $A \ll 1$ corresponds to strong nonlinear effects, whereas $A > 1$ corresponds to weak nonlinearity.

B. NUMERICAL SCHEMES

Four representative time-domain approaches for modeling Eq. (3) are included and compared in the software:

1) A finite-difference explicit conservative algorithm,[15-17] according to which the solution $P(Z_{n+1}, \theta_j) \equiv P_j^{n+1}$ at each subsequent spatial step $n + 1$ is computed for every time grid node j as

$$P_j^{n+1} = P_j^n + \frac{h_Z}{4h_\theta}\left[\left(P_{j+1}^n\right)^2 - \left(P_{j-1}^n\right)^2\right] + \frac{h_Z A}{h_\theta^2}\left(P_{j+1}^n - 2P_j^n + P_{j-1}^n\right), \tag{4}$$

where h_Z and h_θ are spatial and temporal steps, respectively. A template for the numerical scheme, Eq. (4), hereafter referred to as the Conservative scheme, is shown in Fig. 1a.

2) A finite-difference explicit conservative shock-capturing Godunov-type scheme[6,18-22] (Fig. 1b), capable of governing steep shocks in the waveform using a small number of time grid points per shock (approximately 2–3 for plane waves):

$$P_j^{n+1} = P_j^n + \frac{h_Z}{h_\theta}\left(H_{j+1/2}^n - H_{j-1/2}^n\right) + \frac{h_Z A}{h_\theta^2}\left(P_{j+1}^n - 2P_j^n + P_{j-1}^n\right). \tag{5}$$

The fluxes through cell centers $H^n_{j\pm1/2}$ in Eq. (5) are calculated as

$$H^n_{j\pm1/2} = \frac{1}{4}\left[\left(P^+_{j\pm1/2}\right)^2 + \left(P^-_{j\pm1/2}\right)^2\right] + \frac{\max\left|P^+_{j\pm1/2}, P^-_{j\pm1/2}\right|}{2}\left(P^+_{j\pm1/2} - P^-_{j\pm1/2}\right), \tag{6}$$

and the pressures to the right and to the left of the grid point $(n\,, j)$ in Eq. (6) are

$$P^\pm_{j\pm1/2} = P^n_{j\pm1} \mp \frac{h_\theta}{2}\left(\frac{\partial P}{\partial \theta}\right)^n_{j\pm1}, \;\; P^\mp_{j\pm1/2} = P^n_j \pm \frac{h_\theta}{2}\left(\frac{\partial P}{\partial \theta}\right)^n_j. \tag{7}$$

The derivatives $\left(\frac{\partial P}{\partial \theta}\right)^n_{j,j\pm1}$ in Eq. (7) are calculated as follows to increase the stability of the algorithm (5):

$$\left(\frac{\partial P}{\partial \theta}\right)^n_j = \operatorname{minmod}\left(\frac{b\left(P^n_j - P^n_{j-1}\right)}{h_\theta}, \frac{P^n_{j+1} - P^n_{j-1}}{2h_\theta}, \frac{b\left(P^n_{j+1} - P^n_j\right)}{h_\theta}\right), \tag{8}$$

where the value of the weighting coefficient is $1 \le b \le 2$, and

$$\operatorname{minmod}(x_1, x_2, \dots) = \begin{cases} \min\limits_i\{x_i\}, & x_i > 0 \;\; \forall i \\ \max\limits_i\{x_i\}, & x_i < 0 \;\; \forall i\,. \\ 0, & \text{otherwise} \end{cases} \tag{9}$$

Note that $b = 1$ provides more stable operation of the algorithm (5) due to increased numerical dissipation, whereas $b = 2$ yields higher accuracy with minimal dissipation. These schemes are hereafter referred to as the Godunov-type-1 scheme and Godunov-type-2 scheme, respectively.

3) The Austin algorithm, which is a time-domain algorithm based on the exact implicit solution of the lossless Burgers equation (also known as the Riemann solution) combined with interpolation to a uniform time grid (Fig. 1c). The algorithm implements an operator splitting technique[7-10] that treats nonlinear propagation and thermoviscous absorption at each subsequent time step separately. First, the thermoviscous absorption term is solved via the implicit Crank–Nicolson method.[26] Then, an analytical solution is applied to the nonlinear term by shifting the waveform in time according to the local amplitude-dependent propagation speed, using the method of characteristics:[2,23]

$$P(Z + h_Z, \theta) = P(Z, \theta + P \cdot h_Z). \tag{10}$$

The solution is then interpolated back to a uniform time grid.

4) The algorithm specifically designed for solving the lossless Burgers equation in intrinsic coordinates (IC) is hereafter referred to as the IC scheme.[24,25] Equation (3) with $A = 0$, originally formulated in physical coordinates (PC), is transformed into an equivalent equation in IC $(\psi\,, s)$, in which the waveform remains single-valued even when it becomes multivalued in PC (Fig. 1d). The transformation is defined as follows:

$$\psi = \tan^{-1}\left(\frac{\partial P}{\partial \theta}\right), \qquad s = \int_{\theta_0}^{\theta} \sqrt{1 + \left(\frac{\partial P}{\partial \theta}\right)^2}\, d\theta, \tag{11}$$

where $\psi(s)$ is the angle of the tangent to the waveform and s is the arc length along the waveform. In these coordinates, the evolution equation becomes:

$$\frac{\partial \psi}{\partial Z} = \sin^2 \psi + \frac{\partial \psi}{\partial s} \int_0^s \sin\psi \cos\psi \, ds. \tag{12}$$

Equation (12) is solved using a high-order Runge–Kutta method[27] with an adaptive spatial step size h_Z. Thermoviscous absorption is neglected during waveform propagation in intrinsic coordinates. Instead, shocks are introduced into the multivalued physical waveform using the equal area rule[28] after transforming the solution from intrinsic back to physical coordinates. This approach avoids the need for fine temporal discretization within shock regions and allows large spatial steps, making it highly efficient for waveforms with thin shocks, especially in relaxing media.[24,25]

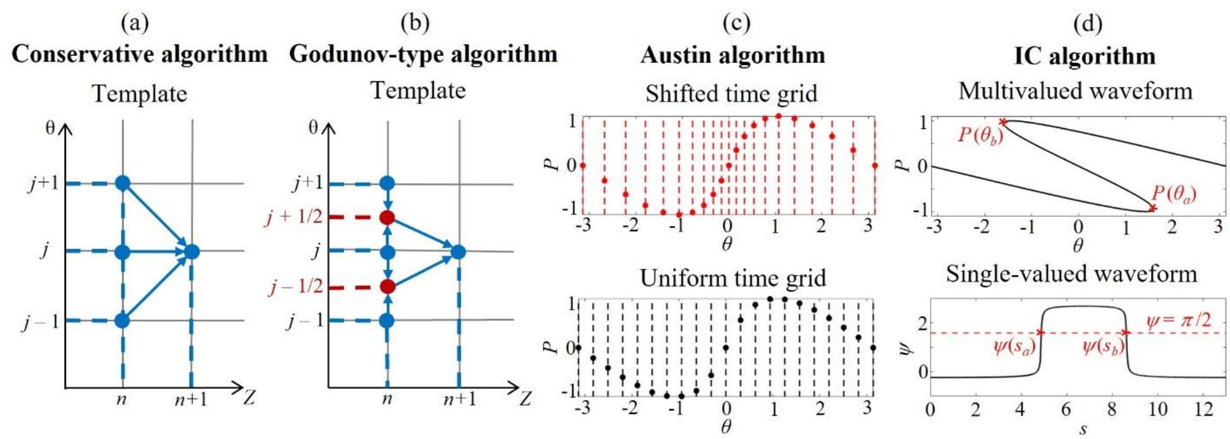

Figure 1. Templates of the numerical schemes implemented in the developed software: a–b – templates for the conservative and shock-capturing Godunov-type algorithms, c – illustration of the interpolation procedure in the Austin algorithm, d – example of a multivalued waveform in physical coordinates and the corresponding single-valued waveform in intrinsic coordinates used in the IC algorithm.

3. SOFTWARE GUI STRUCTURE

The B-Sim software was created using MATLAB App Designer, available in versions starting from R2016a. Since the current project was developed in MATLAB R2023a, we recommend using a MATLAB version that is not significantly older than this one. The application is designed to work within the standard MATLAB environment. No additional toolboxes are strictly required for its core functionality. The open-access code can be downloaded from https://github.com/kvashennikovaav/B-Sim. A manual file is provided with installation instructions and a detailed description of the software.

Below, a brief overview of the software capabilities is presented. The application includes a **Menu** section with drop-down tabs, and a **Help** section containing comprehensive information.

From the **Menu** section, the user can select one of the screens discussed in this section, each providing a different functionality.

The first screen, entitled **Algorithms,** is devoted to a detailed study of the operation of one of the four numerical schemes (Fig. 2). The user can select one of the predefined initial waveforms (a periodic sine wave, one cycle of a sine wave evolving into S and N waves, a shock followed by an exponential tail, or an N wave) and the numerical scheme to be tested. The physical parameters of the problem can also be specified, including the value of A and the maximum propagation distance $Z_{\max}$. In addition, the numerical grid parameters can be set: the spatial step h_Z, the time step h_θ, and the number of time grid points per shock N_{ppsh} used to smooth the initially discontinuous waveforms (the shock followed by an exponential tail and the N wave). This smoothing is required for the present implementation of the IC scheme[24,25] and can also be applied to the other algorithms if A is set to zero. Several recommendations for the choice of the steps h_Z and h_θ and the number of points per shock N_{ppsh} are given in the green fields. They were chosen for each numerical scheme to ensure a compromise between sufficient accuracy compared to the analytical solution and a short run time. General recommendations are marked in blue under the Grid Parameters section. These recommendations are related to stability and accuracy criteria for the numerical schemes under consideration. In the right-hand part of the working screen, the initial waveform (the **Initial Waveform** button), the waveform at a given distance $Z_{\max}$ (the **Waveform at $Z_{\max}$** button) or the waveform evolution (the **Waveform Evolution** button with an opportunity to stop and continue animation with the button **Stop Animation**) can be displayed on a graphic field. The user can also clear the graphic field with **Clear All** button.

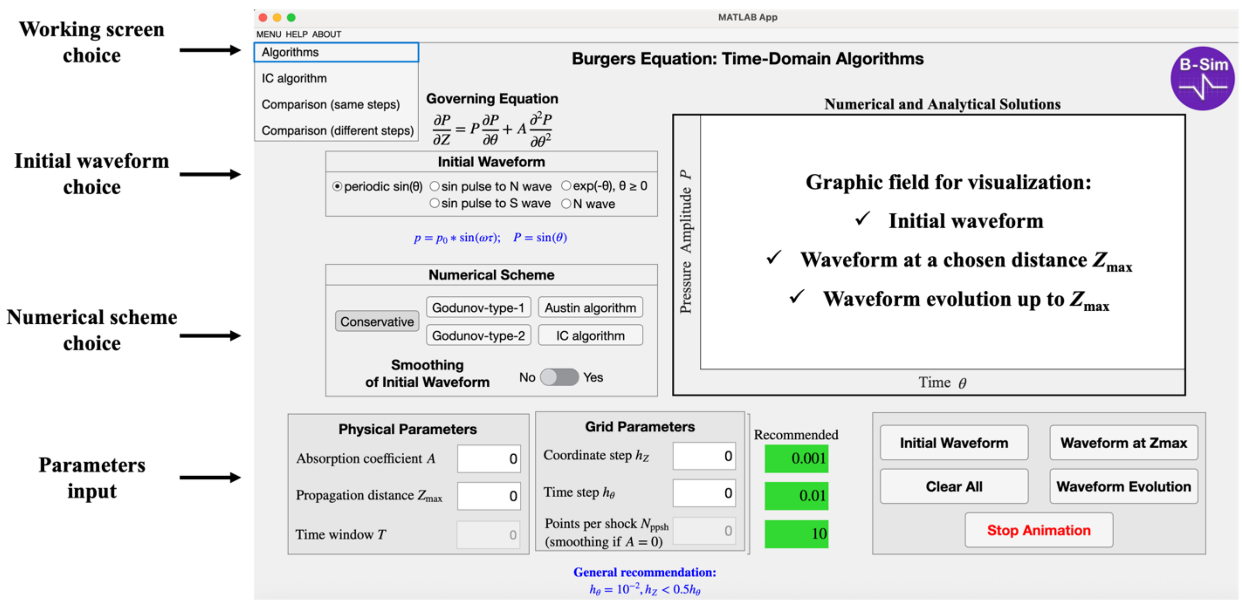

Figure 2. Software graphical window in the Algorithms tab.

The second section, **IC algorithm,** is dedicated to the IC scheme, which is designed for the case of $A = 0$, and therefore the equal area rule[28] is used to account for absorption at the shocks (Fig. 3a, red frame). This panel provides the same options as the **Algorithms** tab. The only difference is that the **IC algorithm** section presents two graphic fields: one shows pressure waveforms in physical coordinates, displaying both multivalued (for $Z > 1$) and single-valued solutions, while the other shows a solution in intrinsic coordinates where it is single-valued.

The third screen, **Comparison (same steps),** allows for a comparative analysis of up to five selected numerical schemes operating with the same grid parameters, either for the waveform at a chosen distance $Z_{\max}$ or during the waveform evolution. The selection of the numerical schemes of interest is performed in the **Numerical Scheme** panel (Fig. 3b), which differs from the panel on the **Algorithms** tab (Fig. 2). Here, one can choose one of the three modes: **not selected** (the scheme is not included in the comparison), **discontinuous initial waveform** (the scheme is included in the comparison without smoothing of the initial waveform), or **smoothed initial waveform** (the scheme is included in the comparison with smoothing of the initial waveform).

Finally, the fourth screen, **Comparison (different steps),** is intended for comparing the results of up to five numerical schemes with temporal and spatial steps specified for each one (Fig. 3c) for the waveform at a chosen distance $Z_{\max}$, with the **Waveform Evolution** button inactive.

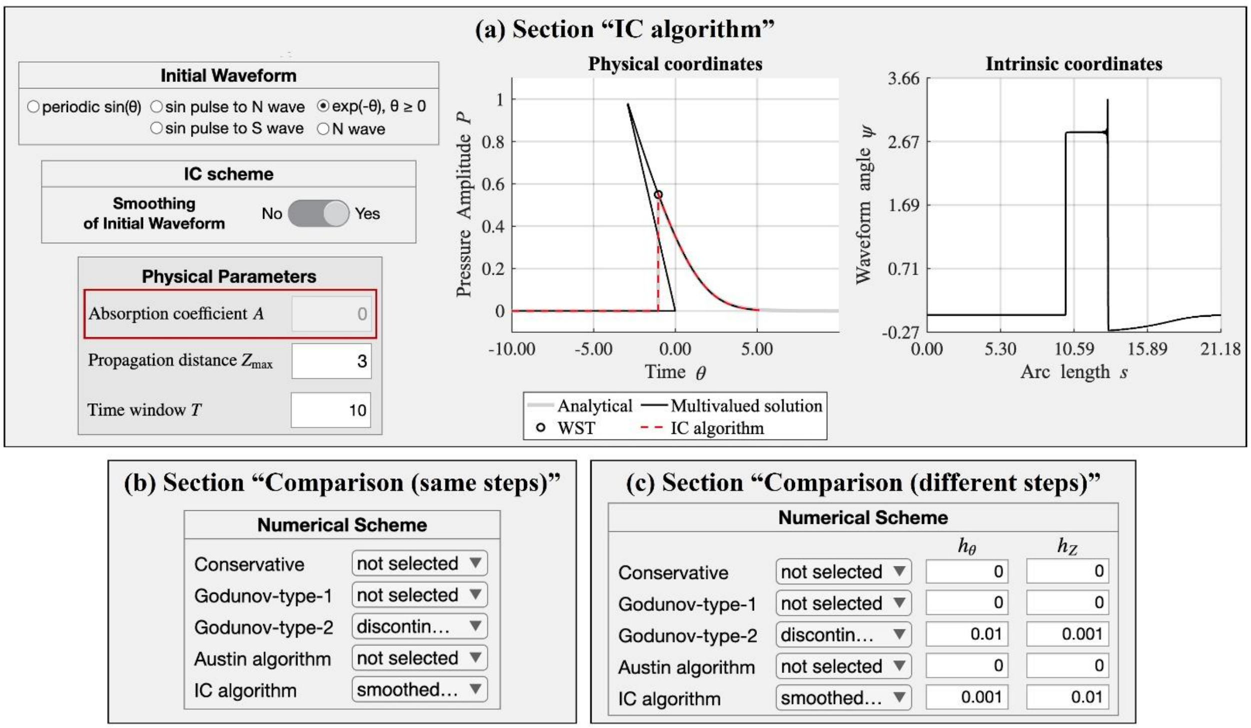

Figure 3. Panels illustrating features that differ from the Algorithms tab: two graphical fields in the IC scheme screen (a); numerical scheme selection panel in the Comparison (same steps) (b) and Comparison (different steps) (c) sections.

4. DISCUSSION AND RESULTS

Figure 4 illustrates the performance of all numerical schemes in simulating the propagation of a periodic sine wave before ($Z_{\max} = 0.5$) and after ($Z_{\max} = 3$) shock formation for the case $A = 0$. The time grid step h_θ was chosen to be the same for all schemes (providing the same number of time grid points) and small enough to ensure correct operation of each numerical algorithm. Spatial steps h_Z were chosen individually for each algorithm following the recommendations from the software. It was determined that $h_\theta = 0.02$ with corresponding h_Z (0.009, 0.002, and 0.018 for the conservative, both Godunov-type, and Austin schemes, respectively; an "average" step for the IC scheme due to its adaptability was equal to 0.0054, with the maximum step limited to 0.01) led to the solution in which the shock amplitude differed from the analytical solution by less than 1% for each chosen scheme. Figure 4 also includes the analytical solution of the Riemann equation (lossless Burgers equation) obtained using the equal area rule[28]. Note that beyond the shock formation distance ($Z > 1$), the conservative scheme becomes unstable and is therefore not shown in Fig. 4b. The results calculated by all schemes look almost identical and differ only in the fine structure of the shock (see "zoom at the shock" in Fig. 4b).

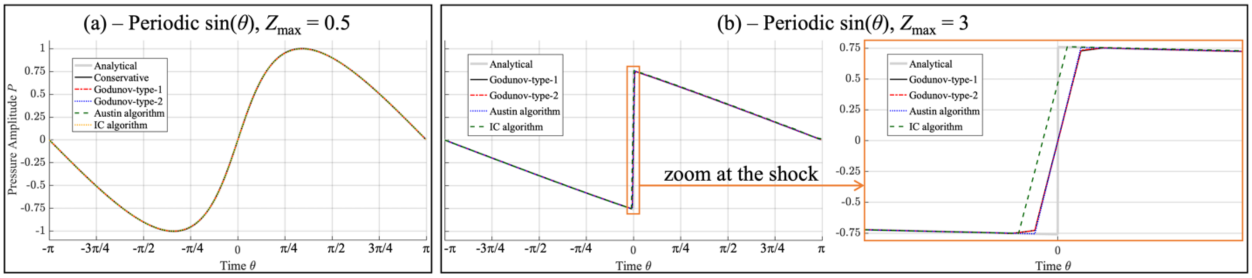

Figure 4. Waveforms (one cycle) of a periodic initially sine wave before (a) and after (b) shock formation, obtained using various numerical schemes and compared with the analytical solution. The simulations were performed for A = 0 with identical temporal and spatial steps for all algorithms.

Table 1 shows a comparison of the calculation times of all algorithms for the selected steps $h_\theta = 0.02$ and h_Z up to the distances $Z_{\max} = 0.5$ and $Z_{\max} = 3$ for the case $A = 0$ when simulating the propagation of the periodic initially sine wave.

Table 1. Runtime of numerical algorithms in B-Sim software (periodic sine wave).

Numerical scheme	**Runtime, s** $\boldsymbol{Z_{\max} = 0.5}$	**Runtime, s** $\boldsymbol{Z_{\max} = 3}$	**Runtime, s** $\boldsymbol{Z_{\max} = 3}$ **with optimized time grid steps**
Conservative	0.004	-	-
Godunov-type-1	0.013	0.050	0.050
Godunov-type-2	0.013	0.050	0.043
Austin	0.002	0.011	0.005
IC	0.031	0.168	0.094

As follows from Table 1, the Austin algorithm turned out to be the most efficient for simulating the considered example of a periodic sine wave propagation before (first column, the Conservative scheme is almost equivalent) and after (second column) shock formation, turning into a sawtooth wave with symmetric shock. It should be noted that the significantly longer runtime of the IC scheme is due to the larger time window required (to ensure correct visualization, seven wave periods are set by default for distances up to $Z_{\max} = 10$, but shorter time windows could be used for smaller propagation distances). The calculations can be optimized (third column) by an appropriate choice of numerical grid parameters – by increasing the time discretization step size and the spatial step accordingly, the Austin and IC schemes become twice as fast.

Figure 5, similar to Figure 4, shows the performance of the numerical schemes for a shock followed by an exponential tail in the case of weak thermoviscous absorption with $A = 0.01$. The IC algorithm is not included in the consideration as it operates with $A = 0$ and accounts for absorption using equal area rule, placing discontinuous shocks that lose accuracy with increased absorption coefficient A. As above, the steps $h_\theta = 0.001$ and corresponding h_Z (0.000045 for the conservative and both Godunov-type algorithms, and 0.0001 for the Austin algorithm) satisfy the accuracy conditions of each numerical algorithm. As a "benchmark" solution, the conservative scheme is used with the temporal and spatial steps mentioned above, the latter of which was decreased until further reduction no longer led to noticeable changes in the solution. In the case of non-zero thermoviscous absorption, the shock front has a finite thickness, which means that numerical calculations using any algorithm are hardly distinguishable, even with a significant increase in the resolution of the shock front region.

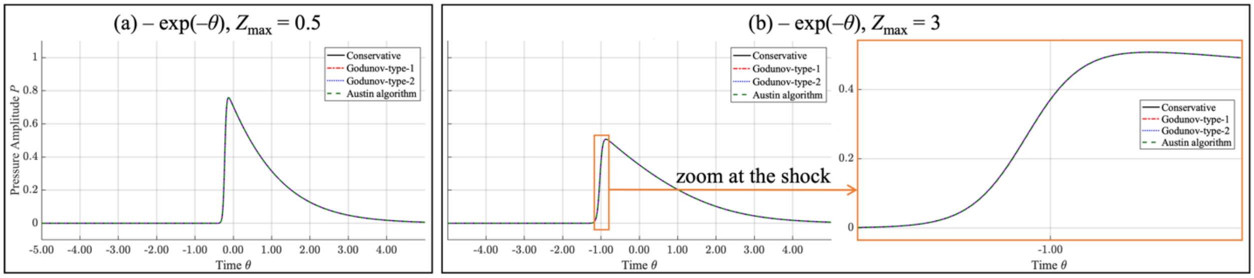

Figure 5. Waveforms of an exponential pulse with a shock before (a) and after (b) shock formation, obtained using various numerical schemes except the IC algorithm. The simulations were performed for A = 0.01 with identical temporal and spatial steps for all algorithms.

Table 2 shows a comparison of the calculation times of all algorithms (except the IC scheme) for the selected steps h_Z and h_θ up to the distances $Z_{\max} = 0.5$ and $Z_{\max} = 3$ for the case $A = 0.01$ when simulating the propagation of the shock followed by an exponential tail.

Table 2. Runtime of numerical algorithms in B-Sim software (a shock followed by an exponential tail).

Numerical scheme	**Runtime, s** $\boldsymbol{Z_{\max} = 0.5}$	**Runtime, s** $\boldsymbol{Z_{\max} = 3}$	**Runtime, s** $\boldsymbol{Z_{\max} = 3}$ **with optimized time grid steps**
Conservative	0.626	3.745	3.745
Godunov-type-1	3.071	18.860	0.124
Godunov-type-2	3.071	18.860	0.124
Austin	1.689	10.295	2.146

From Table 2, considering the shock with exponential tail as an example of a waveform that is initially asymmetrical and thus moves during propagation of the shock, it follows that the conservative scheme is the fastest for simulations up to distances before (first column) and after (second column) shock formation, respectively, only if time grid steps are the same for all algorithms. If the calculations are optimized (third column) by appropriately selecting the numerical grid steps, the runtime for Godunov-type algorithms can be reduced by a factor of a hundred, making them much more efficient than the conservative one. Note that the Austin algorithm is not the fastest in this case of a moving shock, in contrast with the periodic sine wave example, since it requires finer temporal and spatial discretization in order to correctly capture the shock movement.

The two trial examples presented in this paper demonstrate the capabilities of the B-Sim software for efficient comparative analysis of time-domain numerical schemes under different physical propagation conditions. The software provides a platform for evaluating the algorithms' performance in terms of accuracy, computational speed and stability, depending on the presence of thermoviscous absorption and the type of initial waveform. Thus, the B-Sim software can be readily applied for further analysis of other regimes, e.g., moving shocks in the absence of thermoviscous absorption $A = 0$ and symmetric shocks in the media with $A > 0$. Furthermore, the structure of the software allows for the integration of additional physical effects, such as relaxation or geometrical spreading. More detailed comparisons and analyses of specific features of the algorithms will be presented in our subsequent studies.

5. CONCLUSION

The B-Sim GUI software has been developed to simulate the propagation of nonlinear waves with steep shocks. The software solves the Burgers and Riemann (or lossless Burgers) equations in the time domain and enables a comparative analysis of several numerical approaches currently used to model nonlinear effects in shock-wave propagation regimes, including the conservative, the shock-capturing Godunov-type, the Austin algorithm, and intrinsic coordinates (IC) scheme.

It is shown that the optimal choice of a numerical scheme strongly depends on the specific physical problem (the presence of thermoviscous absorption, the type of initial waveform, etc.). For example, in the case of zero thermoviscous absorption, the Austin algorithm is the most efficient in terms of balancing computational accuracy and run time for the modeled example case of the propagation of a periodic sine wave, which exhibits formation of a symmetric shock. In contrast, for the modeled example of a shock followed by an exponential tail that is moving in the retarded time frame during propagation, the Godunov-type scheme provides the fastest performance.

Thus, the developed software is an effective tool for numerical modeling and investigation of nonlinear wave propagation phenomena. Future work could consider the inclusion of additional effects in the tested algorithms, such as geometrical spreading and medium relaxation, which can affect computational efficiency.

ACKNOWLEDGMENTS

The work of the authors affiliated with Moscow State University was supported by the Russian Science Foundation (grant no. 25-12-00157).

REFERENCES

[1] O. A. Sapozhnikov, V. A. Khokhlova, R. O. Cleveland, P. Blanc-Benon, and M. F. Hamilton, “Nonlinear acoustics today,” Acoust. Today **15**(3), 55–64 (2019).

[2] M. F. Hamilton and D. T. Blackstock, eds., *Nonlinear Acoustics*, 3rd ed. (Springer, Cham, Switzerland, 2024).

[3] J. M. Burgers, “A mathematical model illustrating the theory of turbulence,” Adv. in Appl. Mech. **1**, 171–199 (1948).

[4] P. J. Westervelt, “Parametric acoustic array,” J. Acoust. Soc. Am. **35**(4), 535–537 (1963).

[5] E. A. Zabolotskaya and R. V. Khokhlov, “Quasi-plane waves in the nonlinear acoustics of confined beams,” Sov. Phys. Acoust. **15**(1), 35–40 (1969).

[6] P. V. Yuldashev and V. A. Khokhlova, “Simulation of three-dimensional nonlinear fields of ultrasound therapeutic arrays,” Acoust. Phys. **57**(3), 334–343 (2011).

[7] Y.-S. Lee and M. F. Hamilton, “Time-domain modeling of pulsed finite-amplitude sound beams,” J. Acoust. Soc. Am. **97**(2), 906–917 (1995).

[8] R. O. Cleveland, M. F. Hamilton, and D. T. Blackstock, “Time-domain modeling of finite-amplitude sound in relaxing fluids,” J. Acoust. Soc. Am. **99**(6), 3312–3318 (1996).

[9] J. Tavakkoli, D. Cathignol, R. Souchon, and O. A. Sapozhnikov, “Modeling of pulsed finite-amplitude focused sound beams in time domain,” J. Acoust. Soc. Am. **104**(4), 2061–2072 (1998).

[10] V. A. Khokhlova, R. Souchon, J. Tavakkoli, O. A. Sapozhnikov, and D. Cathignol, “Numerical modeling of finite amplitude sound beams: Shock formation in the nearfield of a cw plane piston source,” J. Acoust. Soc. Am. **110**(1), 95–108 (2001).

[11] S. I. Aanonsen, “Numerical computation of the nearfield of a finite amplitude sound beam,” Technical Report 73, Department of Mathematics, University of Bergen, Bergen, Norway, 1983.

[12] M. F. Hamilton, J. Naze Tjøtta, and S. Tjøtta, “Nonlinear effects in the farfield of a directive sound source,” J. Acoust. Soc. Am. **78**(1), 202–216 (1985).

[13] S. S. Kashcheeva, O. A. Sapozhnikov, V. A. Khokhlova, M. A. Averkiou, and L. A. Cram, “Nonlinear distortion and attenuation of intense acoustic waves in lossy media obeying a frequency power law,” Acoust. Phys. **46**(2), 170–177 (2000).

[14] V. A. Khokhlova, A. E. Ponomarev, M. A. Averkiou, and L. A. Crum, “Nonlinear pulsed ultrasound beams radiated by rectangular focused diagnostic transducers,” Acoust. Phys. **52**(4), 481–489 (2006).

[15] R. J. LeVeque, *Finite Volume Methods for Hyperbolic Problems* (Cambridge University Press, 2002).

[16] M. V. Averiyanov, M. S. Basova, and V. A. Khokhlova, “Stationary and quasi-stationary waves in even-order dissipative systems,” Acoust. Phys. **51**(5), 495–501 (2005).

[17] R. D. Richtmyer and K. W. Morton, *Difference Methods for Initial Value Problems*, 2nd ed. (Wiley-Interscience, New York, 1967).

[18] A. Kurganov and E. Tadmor, “New high-resolution central schemes for nonlinear conservation laws and convection-diffusion equations,” J. Comp. Phys. **160**(1), 241–282 (2000).

[19] P. V. Yuldashev, S. Ollivier, M. V. Averiyanov, O. A. Sapozhnikov, V. A. Khokhlova, and P. Blanc-Benon, “Nonlinear propagation of spark-generated N-waves in air: Modeling and measurements using acoustical and optical methods,” J. Acoust. Soc. Am. **128**(6), 3321–3333 (2010).

[20] M. V. Averiyanov, P. Blanc-Benon, R. O. Cleveland, and V. A. Khokhlova, “Nonlinear and diffraction effects in propagation of N-waves in randomly inhomogeneous moving media,” J. Acoust. Soc. Am. **129**(4), 1760–1772 (2011).

[21] O. V. Bessonova and V. A. Khokhlova, “Spatial structure of high intensity focused ultrasound beams of various geometry,” Phys. of Wave Phen. **17**(1), 45–49 (2009).

[22] E. O. Konnova, V. A. Khokhlova, and P. V. Yuldashev, “The use of graphic accelerators in simulation of nonlinear ultrasonic beams with shock fronts on the basis of the Westerwelt equation,” Acoust. Phys. **68**(6), 529–536 (2022).

[23] O. V. Rudenko and S. I. Soluyan, *Theoretical Foundations of Nonlinear Acoustics* (Nauka, Moscow, 1975).

[24] W. A. Willis, J. M. Cormack, and M. F. Hamilton, “Use of intrinsic coordinates to simulate the evolution of shocks in multirelaxing fluids,” J. Acoust. Soc. Am. **157**(5), 3824–3835 (2025).

[25] W. A. Willis III, *Coalescence of Nonlinear Acoustic Waves, with Application to Supersonic Jet Noise*, Ph.D. Dissertation, The University of Texas at Austin, Austin, Texas (2024).

[26] W. F. Ames, *Numerical Methods for Partial Differential Equations*, 3rd ed. (Academic Press, New York, 1992).

[27] J. R. Dormand and P. J. Prince, “A family of embedded Runge-Kutta formulae,” J. Comput. Appl. Math. **6**(1), 19–26 (1980).

[28] L. D. Landau, “On shock waves at large distances from the place of their origin,” J. Phys. USSR **9**(6), 496–500 (1945).